J Physiol (2003), **552.1**, *pp.* 135–148

DOI: 10.1113/jphysiol.2003.047191
www.jphysiol.org

Journal of Physiology

Role of the hyperpolarization-activated cation current (I_h) in pacemaker activity in area postrema neurons of rat brain slices

Makoto Funahashi, Yoshihiro Mitoh, Atsushi Kohjitani* and Ryuji Matsuo

*Departments of Oral Physiology and *Dental Anesthesiology, Okayama University Graduate School of Medicine and Dentistry, 2-5-1 Shikata-cho, Okayama 700-8525, Japan*

To clarify the functional properties of the hyperpolarization-activated cation current (I_h) as a pacemaker current in area postrema neurons, whole-cell recordings were made in visually identified cells in rat brain slices. The activation of I_h was identified in approximately 62 % of area postrema neurons tested. The cells displaying I_h showed a depolarizing 'sag' in responses to hyperpolarizing current injection in current-clamp mode. The reversal potential for the I_h was −36 mV, and this was shown to depend on the external concentration of Na^+ and K^+ ions. Extracellular Cs^+ ions (2 mM) and ZD7288 (100 μM), a potent selective I_h channel antagonist, blocked I_h and induced a membrane potential hyperpolarization, suggesting the sustained activation of I_h near the resting potential and a contribution from I_h to membrane potential maintenance at more depolarized levels. In contrast, extracellular Ba^{2+} ions caused a depolarization of the membrane potential, suggesting the blockade of inward rectifier K^+ currents. ZD7288 decreased the spontaneous discharge rate by prolonging the slow depolarization between two spikes, with minimal effect on the amplitude of the after-hyperpolarization or action potential waveforms. I_h stabilized the latency of rebound action potentials. I_h was weakly activated by external 8-bromoadenosine 3′,5′ cyclic monophosphate (1 mM) or forskolin (50–100 μM), indicating that the I_h channel subtypes in area postrema cells could be modulated by intracellular cAMP. Our findings indicate that I_h contributes to the subthreshold membrane and firing properties of rat area postrema neurons and may regulate their resting membrane potential and firing patterns.

(Resubmitted 13 May 2003; accepted after revision 24 July 2003; first published online 1 August 2003)
Corresponding author M. Funahashi: Department of Oral Physiology, Okayama University Graduate School of Medicine and Dentistry, 2-5-1 Shikata-cho, Okayama 700-8525, Japan. Email: mfuna@md.okayama-u.ac.jp

The area postrema is a midline structure at the caudal end of the fourth ventricle. It has been implicated as an important central structure involved in the regulation of many autonomic functions including the control of food intake (Contreras *et al.* 1984; van der Kooy, 1984; Ritter *et al.* 1986), body fluid homeostasis (Miselis *et al.* 1987; Iovino *et al.* 1988) and cardiovascular regulation (Ferguson & Smith, 1991). The area postrema is also well known as a trigger zone for the vomiting reflex in cats and dogs (Borison & Wang, 1953). Although rats do not vomit, many studies indicate that the area postrema in this species has functional relevance in conditioned taste or drug-induced aversion learning associated with nausea (Berger *et al.* 1973; Coil & Norgren, 1981; Gallo *et al.* 1990).

The area postrema is one of the circumventricular organs that lack a blood–brain barrier, offering specific central neural components unique access to circulating substances. Therefore, many studies *in vivo* and *in vitro* have evaluated the chemosensitivity of area postrema neurons to various chemical substances (Barnes *et al.* 1988; Carpenter *et al.* 1988; Funahashi & Adachi, 1993; Allen & Ferguson, 1996). Recently, patch-clamp techniques were used to investigate the regulation of membrane excitability in area postrema neurons (Hay & Lindsley, 1995; Hay *et al.* 1996; Jahn *et al.* 1996; Li & Hay, 2000; Funahashi *et al.* 2002*a*,*b*). We were the first to describe a hyperpolarization-activated cation current (I_h) in area postrema neurons (Funahashi *et al.* 2002*b*). In the present study, we sought to define the functional significance of I_h for area postrema neuronal activity.

I_h has been identified in the sinoatrial node cells of the heart (Brown *et al.* 1977; Yanagihara & Irisawa, 1980; DiFrancesco, 1981) as a 'funny' current (I_f), and was named for its peculiar characteristic of anomalous rectification. I_h contributes to the generation of the slow depolarization in cardiac pacemaker cells. The activation of I_h in central neurons was first reported in hippocampal pyramidal cells (Halliwell & Adams, 1982) where it was called I_q (q for 'queer'). Subsequently, I_h channels have been described in various central and peripheral neurons (e.g. Pape, 1996). I_h also contributes to pacemaker activity in neurons (e.g. specific contributions to rhythmic-oscillatory activity in

thalamic relay neurons; McCormick & Pape, 1990*a*; Pape, 1996; Luthi & McCormick, 1998), hippocampal CA1 interneurons (Maccaferri & McBain, 1996) and pyramidal cells (Gasparini & DiFrancesco, 1997), neurons of the hypoglossus nucleus and the pre-Bötzinger complex in the medulla oblongata (Thoby-Brisson *et al.* 2000) and cells of the entorhinal cortex (Dickson *et al.* 2000).

The common properties of I_h are: (1) slow activation by membrane hyperpolarization more negative than resting potential (e.g. −60 to −70 mV) without any inactivation state, (2) selective conductance for Na^+ and K^+ and (3) sensitivity to extracellular Cs^+ but not to Ba^{2+}. The physiological roles of I_h for excitability in central neurons have been reported as: (1) the depolarizing 'sag' in response to hyperpolarizing current injection representing the activation of I_h during current-clamp recordings, (2) modulation of the afterhyperpolarization (AHP)-like potential at the termination of depolarizing current injection and (3) contribution to the resting potential (Pape, 1996).

Molecular biological studies have identified the gene family of I_h channels, which are termed hyperpolarization-activated cyclic-nucleotide-gated (HCN) channels, in mouse, human and sea urchin sperm (see review by Biel *et al.* 1999). The HCN family of I_h channels could be further divided into four subtypes (HCN1–HCN4) in both the mouse and human. All subtypes of HCN have a cyclic-nucleotide binding domain in the cytosolic C-terminus, but their properties and cellular distribution vary. The activation of HCN2 is highly accelerated by increases of cytoplasmic cAMP. By contrast, HCN1 is only weakly modulated by cAMP. HCN2 is highly expressed in thalamic neurons (Monteggia *et al.* 2000; Santoro *et al.* 2000). This is consistent with electrophysiological demonstrations of increases in I_h amplitude after extracellular application of 8-bromoadenosine 3′,5′ cyclic monophosphate (8Br-cAMP) or forskolin to thalamic neurons (McCormick & Pape, 1990*b*; Pape, 1992). HCN1 and HCN3 channels were suggested to be the predominant forms in area postrema neurons (Monteggia *et al.* 2000). As such, the activation of I_h channels in area postrema neurons would be expected to depend less on the cAMP system, similar to HCN1 channels in the hippocampal CA1 neurons (Biel *et al.* 1999). There are, however, no electrophysiological data to address this suggestion.

In the present study, we performed patch-clamp recordings to examine the ionic nature and pharmacological properties of I_h and the effects of activation and deactivation of I_h on the subthreshold membrane properties and generation of action potentials. We introduce experimental evidence for a pacemaking function of I_h in area postrema neurons.

METHODS

Slice preparation and maintenance

The experimental protocols used were approved by the Okayama University Animal Use Committee. Brain slices were prepared from Sprague-Dawley albino rats (7–21 days postnatal) as described previously (Funahashi *et al.* 2002*a*,*b*). Animals were anaesthetized with halothane and decapitated. Each brain was rapidly removed from the skull and kept for 1 min in ice-cold, oxygenated sucrose Ringer solution containing (mM): 234 sucrose, 2.5 KCl, 0.5 $CaCl_2$, 10 $MgSO_4$, 1.25 NaH_2PO_4, 26 $NaHCO_3$ and 10 glucose, at pH 7.4 when exposed to 95 % O_2–5 % CO_2. Coronal brainstem slice preparations (150–200 μm thick) that included the area postrema were obtained using a tissue slicer (Dosaka EM, Kyoto, Japan). The brain slices were incubated for more than 1 h in oxygenated artificial cerebrospinal fluid (normal ACSF) containing (mM): 124 NaCl, 5 KCl, 2.0 $CaCl_2$, 1.6 $MgCl_2$, 26 $NaHCO_3$ and 10 glucose, at pH 7.4 when exposed to 95 % O_2–5 % CO_2 at room temperature (24–27 °C). After preincubation, the slices were transferred to a recording chamber on an upright microscope (DMLFS, Leica). The slices were continuously perfused with ACSF at room temperature (24–27 °C) at the rate of 2–3 ml min^{-1} using a peristaltic pump (Minipuls 2, Gilson, Villiers, France).

Recording technique and data analysis

Whole-cell patch-clamp recordings were obtained from area postrema neurons that were visualized with Nomarski optics using a × 40 water-immersion objective. The patch pipettes had resistances of 5–8 MΩ when they were filled with a solution containing (mM): 135 potassium gluconate, 10 KCl, 1 $MgCl_2$, 10 Hepes, 0.2 EGTA, 2 Na_2ATP and 0.1 spermine, adjusted to pH 7.3 with KOH. In some cells, where we tested the effects of cAMP, perforated patch recordings were made using amphotericin B. In this case, the patch-pipettes were filled with a solution containing (mM): 150 KCl and 10 Hepes, adjusted to pH 7.3 with KOH. Amphotericin B solubilized preparation (Sigma, St Louis, MO, USA) was added into the pipette solution just before use. The final concentration of amphotericin B in the pipette solution was 300 μg ml^{-1} (Rae *et al.* 1991).

Signals were amplified by an Axopatch-200A amplifier (Axon Instruments, Foster City, CA, USA) and filtered at 5 kHz. The series resistance was less than 22 MΩ and compensated up to 70 %. Recordings in which the series resistance changed by more than 10 % of the initial value were not included in the analysis. Measurements were acquired using the pCLAMP system (Axon Instruments) and stored on a computer hard disk for off-line analysis. The liquid junction potential between the ACSF and the internal solution was approximately −10 mV in this study. The actual membrane potential was corrected by this value. Off-line analysis was performed using Axograph software (Axon Instruments). All values described in the present study are expressed as means ± S.E.M. Student's *t* test was employed for statistical analysis.

To evaluate the effect of the potent selective I_h channel antagonist ZD7288 on I_h, the obtained data were fitted by the function: $I/I_{cont} = (1 + ([ZD7288]/m)^n)^{-1}$, where I_{cont} is the current in the control solution, [ZD7288] is the concentration of ZD7288, m is the value of IC_{50}, and n is the Hill coefficient.

Solutions

Current-clamp recordings were routinely performed in normal ACSF. Voltage-clamp recordings were usually made in a modified ACSF containing (mM): 104 NaCl, 20 TEA, 5 KCl, 1 $BaCl_2$, 1.6

$MgSO_4$, 26 $NaHCO_3$, 2 4-aminopyridine (4-AP), 0.001 TTX and 10 glucose, except some experiments in which both current-clamp and voltage-clamp recordings were taken from the same cells. Some voltage-clamp recordings were taken in the normal ACSF containing TTX (1 μM). The effect of extracellular Cs^+ and Ba^{2+} was examined by the addition of CsCl (2 mM) and $BaCl_2$ (1 mM) to normal ACSF. To alter the concentration of K^+ ions, KCl was substituted for equimolar NaCl in the perfusate. To make a low-sodium perfusate, choline chloride or mannitol was added as a substitute for equimolar NaCl. TTX was obtained from Wako Pure Chemical (Osaka, Japan) and TEA, 4-AP, 8Br-cAMP, SQ22536 and forskolin were from Sigma. ZD7288 was kindly provided by Astra Zeneca (Osaka, Japan). All other reagents were from Nacalai Tesque, Osaka, Japan.

RESULTS

I_h was observed in more than 60 % of all area postrema neurons tested. The data presented here are based on recordings from 160 cells displaying I_h. A representative sample of 28 cells showed a resting membrane potential of −63.5 ± 0.8 mV (range of −57 to −69 mV). The mean input resistance was 432.4 ± 16.3 MΩ (n = 30). Overshooting action potentials were observed in all cells recorded in current-clamp mode.

Cells displaying I_h usually showed various amplitudes of the fast transient outward current (fast I_{to}), but no cells displaying I_h showed the slow transient outward current (slow I_{to}) (Funahashi *et al.* 2002*a*,*b*). In the present study, voltage-clamp recordings were routinely performed in the modified ACSF to minimize the contamination of I_h. Figure 1*A* shows typical recordings of I_h in an area postrema neuron during activation voltage protocols in a modified ACSF that contained TEA (20 mM; blocking the delayed rectifier K^+ current), $BaCl_2$ (1 mM; blocking the inward rectifier K^+ current, I_{Kir}), 4-AP (2 mM; blocking the transient outward K^+ current), TTX (1 μM; blocking the Na^+ current) and nominally zero Ca^{2+} (0 mM $CaCl_2$; preventing Ca^{2+} influx). Hyperpolarizing step pulses of 1 s duration between −40 and −130 mV (10 mV decrements) were used as the activation voltage protocols. The holding potential was −60 mV in this and subsequent voltage-

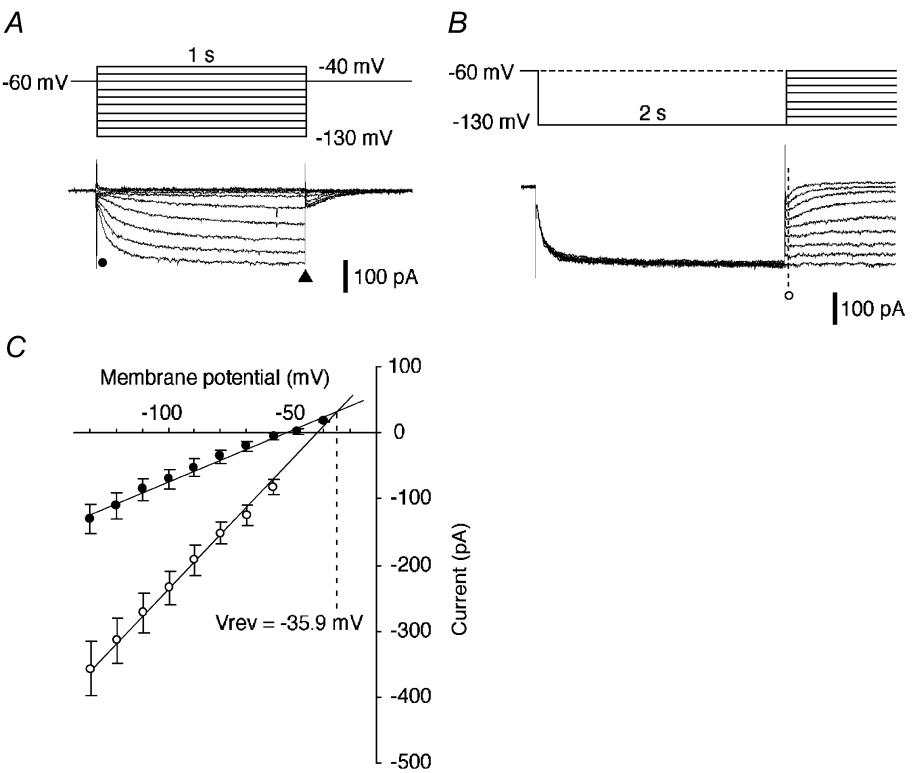

Figure 1. Estimating the reversal potential (I_{rev}) of I_h in area postrema neurons

A, slowly activated inward current elicited by hyperpolarizing step pulses (upper traces). Interval between voltage step commands: 3 s in this and subsequent figures. The holding potential was −60 mV in this and subsequent voltage-clamp recordings. An 'instantaneous' current (I_{in}) was measured at the point marked ●. A 'steady state' current (I_{ss}) was measured at the end of the voltage steps (▲). *B*, hyperpolarizing prepulses and following step pulses (upper traces) elicited deactivation of I_h. The interval between voltage step commands was 4 s; I_{in} was measured at the point marked ○. *C*, plots of I_{in} obtained in the experiments shown in *A* (●) and *B* (○) against the membrane potential (n = 19). The dashed line indicates the value of the membrane potential (−35.9 mV) at the intersection of the two regression lines, which corresponds to the V_{rev} of I_h. All recordings were made in ACSF containing TEA, Ba^{2+}, 4-AP, TTX and nominally zero Ca^{2+} (see Methods).

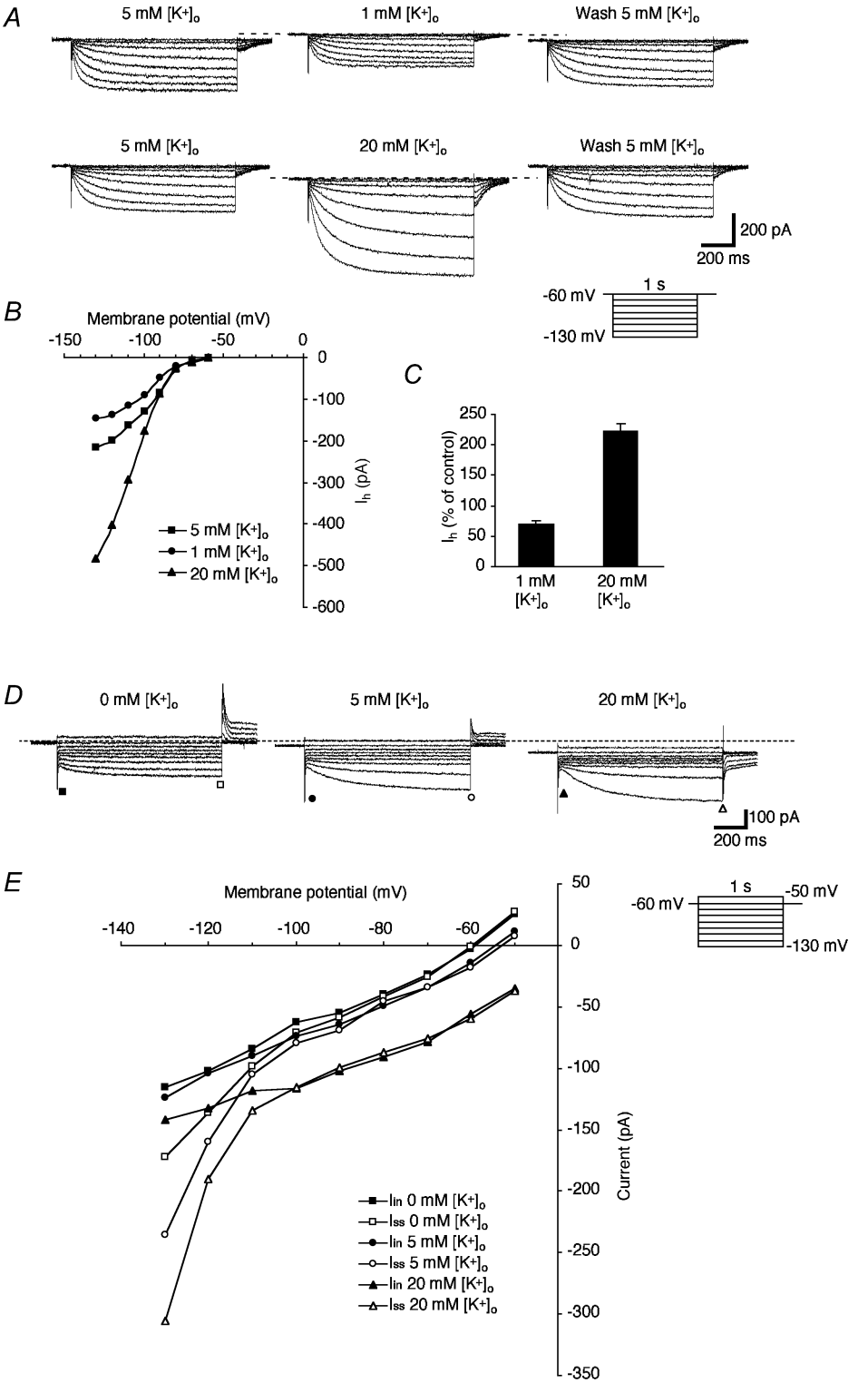

Figure 2. Effects of changing the $[K^+]_o$ on I_h

A, currents elicited by hyperpolarizing voltage steps (1 s duration, from −60 to −130 mV with 10 mV decrements) in three different $[K^+]_o$ (1, 5 and 20 mM). The control ACSF contained 5 mM K^+. All solutions contained TEA, Ba^{2+}, 4-AP, TTX and nominally zero Ca^{2+}. Note the outward and inward shifts of the holding current with 1 and 20 mM of $[K^+]_o$, respectively. *B*, plots of the amplitude of I_h elicited at each value of $[K^+]_o$. *C*, mean values for the effects of changing $[K^+]_o$ on I_h ($n = 5$). The conductance of I_h, estimated by calculation of the slope for each plot between −80 and −130 mV of the membrane potential, was compared with the control level. *D*, current elicited by voltage steps (1 s duration, from −50 to −130 mV with 10 mV decrements) in the low-Na^+ solution containing TTX (1 μM) and three different concentrations of K^+ (1, 5 and 20 mM). NaCl was substituted for choline chloride and K^+ was simply added in the perfusate. *E*, plots of

clamp recordings. The amplitude of I_h was obtained by subtraction of the instantaneous currents (I_{in}, Fig. 1*A*, ●) at the end of the capacitive current transient (5–10 ms after stimulus onset) from the steady-state currents at the end of the 1 s voltage step (I_{ss}, Fig. 1*A*, ▲). The mean amplitude of I_h at the −130 mV command voltage was 293 ± 20 pA (n = 21).

To confirm the kinetic properties, we assessed the activation curve and the time course of I_h using the same method as described in our previous paper (Funahashi *et al.* 2002*b*). This assessment yielded an activation range of I_h conductance between −60 and −130 mV, with a half-activation voltage ($V_{½}$) of −96.1 ± 2.6 mV and slope value (k) of 9.8 ± 0.4 (n = 10), and the time constant for activation of I_h ranged from 309 ± 55 ms at −70 mV to 63 ± 15 ms at −130 mV (n = 10). There was no significant difference between these values and those reported in our previous study ($P > 0.05$). For more details of the kinetic properties of I_h, the reader is referred to our previous paper (Funahashi *et al.* 2002*b*).

The reversal potential of I_h was determined using a modification of the procedure described by Bayliss *et al.* (1994; see Fig. 1*B*). The protocol used a prepulse of 2 s duration at −130 mV followed by test steps to potentials between −130 and −60 mV (10 mV decrements). As shown in Fig. 1*B*, the instantaneous currents elicited by this protocol indicate leak currents plus I_h. The I_{in} elicited by this voltage protocol, as shown in Fig. 1*B* (○), were plotted against the membrane potential (Fig. 1*C*). I_{in} as shown in Fig. 1*A* (●) was also plotted as a function of membrane potential (Fig. 1*C*). Both plots in Fig. 1*C* were well fitted with linear regression. The reversal potential of I_h was estimated by calculation of the membrane potential at the intersection of these two regression lines. The reversal potential was found to be −35.5 mV in this particular cell and −35.9 ± 3.5 mV in a large sample (n = 19), consistent with the participation of both Na^+ and K^+ conductances.

Effects of changing $[K^+]_o$ and $[Na^+]_o$ on I_h

It has been reported that in other central neurons, I_h is carried by both Na^+ and K^+ (Pape, 1996). The reversal potential of I_h (about −36 mV) in the present study also suggested that I_h could be carried by a mixture of both Na^+ and K^+. To investigate the ionic basis of I_h, we tested the effects of changing $[K^+]_o$ and $[Na^+]_o$ on I_h. Decreasing $[K^+]_o$ from 5 to 1 mM resulted in an outward shift of the holding current, a marked decrease in the amplitude of I_{ss} and an attenuation of I_h, as measured by the difference between I_{ss} and I_{in} (Fig. 2*A*, upper panel and *B*). Raising $[K^+]_o$ from 5 to 20 mM produced an inward shift of the holding current, a marked increase in the amplitude of I_{ss} and an enhancement of I_h, as measured by the difference between I_{ss} and I_{in} (Fig. 2*A*, lower panel and *B*). The reversal potentials in this cell, as assessed by the same method mentioned above, were −37 and −25 mV in 5 and 20 mM $[K^+]_o$ solutions, respectively. The mean value of the shift in the reversal potential produced by an increase in $[K^+]_o$ from 5 to 20 mM, was 12 ± 2.5 mV (n = 5). The amplitudes of I_h, calculated as the difference between I_{ss} and I_{in} at each $[K^+]_o$, were plotted against the membrane potential (Fig. 2*B*). The conductance of I_h at each $[K^+]_o$ was estimated by calculating the slope for each plot at membrane potentials between −80 and −130 mV (Maccaferri *et al.* 1993). The conductance of I_h obtained by this method decreased to 69 ± 5.5 % of the control level during exposure to 1 mM $[K^+]_o$ and increased to 221 ± 12 % of the control level during exposure to 20 mM $[K^+]_o$ (Fig. 2*C*, n = 5 in each condition). Both changes were statistically significant ($P < 0.01$). The equilibrium potentials of K^+ (E_K) defined by the Nernst equation were −128, −87 and −51 mV for 1, 5 and 20 mM $[K^+]_o$, respectively. The driving force values for the K^+ current calculated using the values of E_K were 2, 43 and 79 mV at a −130 mV command voltage. Since the driving force for the K^+ current during exposure to 1 mM $[K^+]_o$ was essentially zero, the entire I_h in this medium should be carried by Na^+, as indicated in Fig. 3. The driving force for an inward K^+ current at −130 mV proportionally increased with increases in $[K^+]_o$ to 5 or 20 mM. The apparent increase in conductance (resulting from the increased current at the same voltage) during exposure to 5 and 20 mM $[K^+]_o$ is principally a result of the additional current through the channel carried by K^+. If the I_h channel is relatively more permeable to K^+, then conditions that permit a larger fraction of the current to be carried by K^+ (such as increased $[K^+]_o$) would also be associated with larger total currents. In low $[K^+]_o$, a Goldman-type rectification is expected since K^+ is less available as a charge carrier. Alternatively, a larger current during conditions of high $[K^+]_o$ could be due to $[K^+]_o$-dependent changes in the permeability ratio of Na^+ to K^+ (P_{Na}/P_K), as suggested in previous studies (Hestrin, 1987; Frace *et al.* 1992; see Discussion). These results indicate that K^+ ions can mediate a significant component of I_h.

Changes in K^+ ion concentrations were also tested in media where the Na^+ ions were completely replaced with an equimolar amount of choline ions (Fig. 2*D* and *E*). Raising $[K^+]_o$ from 0 to 5 to 20 mM produced an inward current and a marked increase in the amplitude of I_h at membrane potentials of −120 and −130 mV, as measured by the difference between I_{ss} and I_{in} (Fig. 2*D* and *E*, n = 4).

I_{in} (■, ●, ▲) and I_{SS} (□, ○, △) obtained from current traces in each $[K^+]_o$ as a function of the membrane potential. Note a marked increase in the amplitude of I_h at more negative membrane potentials (< −100 mV) and the dose-dependent inward shift of the holding current.

The tail currents, which were outward at 0 and 5 mM $[K^+]_o$, changed to inward currents in the perfusate containing 20 mM $[K^+]_o$ and low Na^+, again suggesting a substantial contribution by K^+ to I_h.

Decreasing $[Na^+]_o$ from 150 to 50 mM resulted in a marked reduction of the amplitude of I_{ss} and a relatively slower time course of activation of I_h (Fig. 3*A*). The amplitudes of I_{ss} and I_{in} during each condition of $[Na^+]_o$ were plotted against membrane potential (Fig. 3*B*). These plots revealed decreases in the amplitude of I_{ss} at every membrane potential between −70 and −130 mV and no significant change in I_{in} (Fig. 3*B*). The reversal potentials in this cell, as assessed by the same method as shown in Fig. 1, were −38 and −57 mV in 150 and 50 mM $[Na^+]_o$ solutions, respectively. The mean change of the reversal potential in the hyperpolarizing direction was 18 ± 2 mV ($n = 4$). These findings indicate that Na^+ ions also significantly contribute to I_h.

Sensitivity of I_h to Cs^+ and ZD7288

It has been reported that the extracellular application of Cs^+ in the millimolar concentration range blocks I_h in the pacemaker cells of the heart (DiFrancesco, 1982) and various central neurons in the brain (Halliwell & Adams, 1982; Pape, 1996). As shown in Fig. 4*A*, bath application of CsCl (2 mM) caused marked decreases in the amplitudes of I_{ss} and tail currents, and minimal decreases in the leak and capacitive currents ($n = 7$ cells). Cs^+-sensitive currents were isolated by subtraction of the currents in the presence of Cs^+ from currents in the control solution. Thus isolated, it was clear that most of the time-dependent current evoked by hyperpolarization was strongly sensitive to external Cs^+ (Fig. 4*A*, right panel).

To investigate the contribution of the Cs^+-sensitive currents to the resting membrane potential, we examined the effects of extracellular Cs^+ (2 mM; $n = 4$ cells) on the membrane potential using a current-clamp recording without continuous DC current injection (McCormick & Pape, 1990*a*; Maccaferri *et al.* 1993; Travagli & Gillis, 1994). The input resistance was monitored by injection of hyperpolarizing current pulses (160 pA, 100 ms duration) once every 5 s. A typical recording is shown in Fig. 4*B*1. The input resistance was markedly increased by the application of CsCl in the extracellular perfusate and returned to control levels after washing ($n = 4$ cells). The magnified trace of the membrane potential shown in Fig. 4*B*2 clearly shows the hyperpolarization of the membrane potential from −61 to −66 mV, which is coincident with the presence of extracellular Cs^+. The mean magnitude of hyperpolarization was 5.2 ± 0.85 mV ($n = 4$). Figure 4*B*3 shows responses to hyperpolarizing current pulses injected before, during and after the

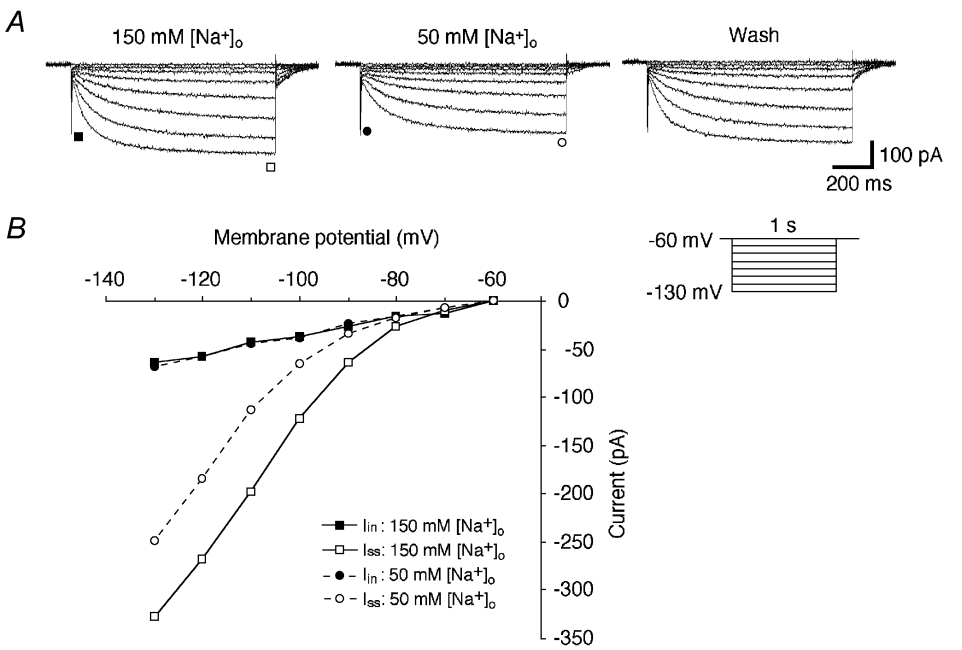

Figure 3. Effects of changing $[Na^+]_o$ on I_h

A, currents elicited by hyperpolarizing voltage steps (inset) in control solution containing 150 mM Na^+ (left panel), during reduction of $[Na^+]_o$ (50 mM, middle panel) and during washout with the control solution (right panel). Choline chloride was added as an equimolar substitute for NaCl. All recordings were made in the presence of TTX (1 μM). Note the decrease in the amplitude of I_{ss} and the slower time course of I_h activation during the low-Na^+ solution. *B*, plots of I_{in} (■, ●) and I_{ss} (□, ○) obtained from current traces in *A* as a function of the membrane potential. Note a marked decrease in the amplitude of I_{ss} with no significant changes in the amplitude of I_{in} during recording with the low-Na^+ solution.

application of CsCl, corresponding to *a, b* and *c* shown in Fig. 4*B*1. The disappearance of the voltage 'sag' and a marked increase in membrane resistance also accompanied the application of CsCl. These findings suggest that I_h is activated around the resting membrane potential (e.g. −61 mV) and would contribute to maintaining the membrane potential at more depolarized values.

We next examined the sensitivity of hyperpolarization-activated currents in area postrema neurons to ZD7288, a potent selective I_h channel antagonist (BoSmith *et al.* 1993; Harris & Constanti, 1995; Gasparni & DiFrancesco, 1997). As shown in Fig. 5*A*, the bath application of ZD7288 (10, 20, 50, 100 and 200 μM) suppressed the activation of I_h in a dose-dependent manner ($n = 6$). ZD7288 reduced the amplitude of I_{ss} with only a small effect on I_{in}. A decrease in the amplitude of I_h was observed at all membrane potentials between −60 and −130 mV in all cells tested (data not shown). The values of IC_{50} and the Hill coefficient were 23.1 μM and 1.8, respectively, suggesting co-operativity of action. These results suggest that ZD7288 suppressed the activation of I_h in a dose-dependent manner.

We tested the effects of I_h blockade on spontaneous firing by area postrema neurons. As shown in Fig. 5*B* and *C*, the bath application of ZD7288 (100 μM) decreased the spontaneous discharge rate to 54.6 ± 5.8 % of the control level ($n = 6$). ZD7288 did not change the action potential waveform properties but made the time course of the depolarization during the AHP phase slower towards the firing threshold (Fig. 5*Bc*). The mean values for the slope steepness in this cell before and during the application of ZD7288 were 29 ± 8 and 18 ± 5, respectively ($n = 7$ epochs in each). The mean values for the slope steepness significantly decreased to 61 ± 7 % of the control level during the application of ZD7288 ($P < 0.01$, $n = 6$ cells). Although ZD7288 caused changes in action-potential-related phenomena such as the AHP, much of the firing

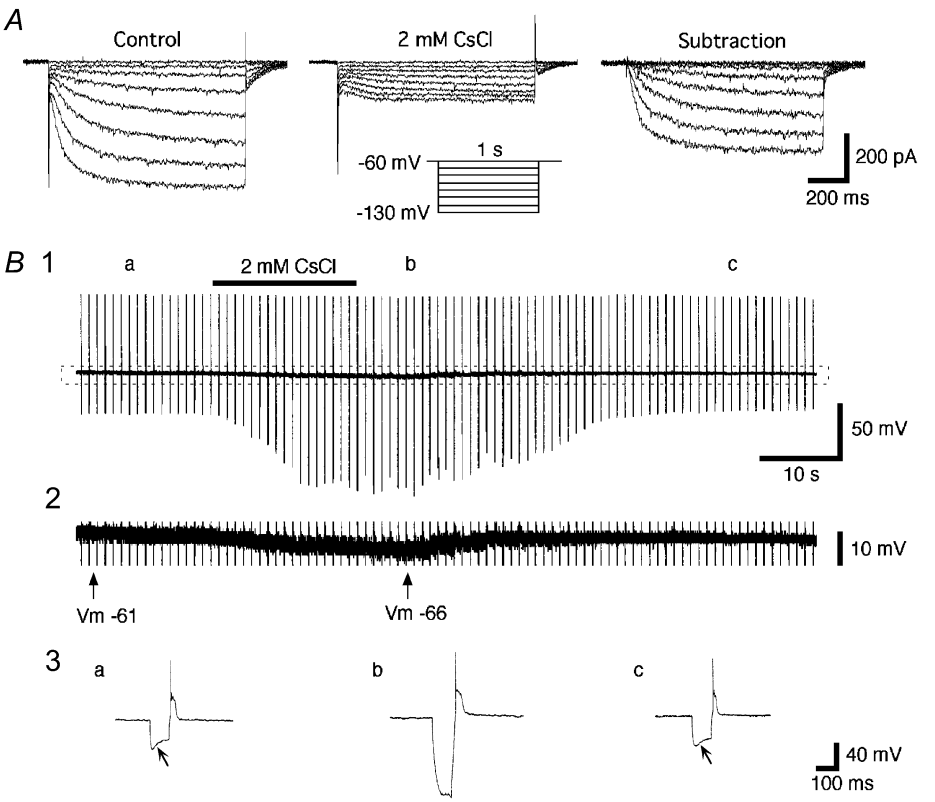

Figure 4. Extracellular Cs^+ blocks I_h

A, currents elicited by hyperpolarizing voltage steps (inset) in control (modified ACSF, left panel) and after addition of extracellular CsCl (2 mM, middle panel). The Cs^+-sensitive current was isolated by digital subtraction (right panel). *B*1, recordings of the membrane potential and input resistances before, during and after the bath application of CsCl (2 mM). The bar above the trace indicates the period of the application of CsCl. The input resistance was measured by injection of hyperpolarizing current pulses (160 pA, 100 ms duration) once every 5 s. Note the marked increases in input resistance induced by the extracellular Cs^+. *B*2, an enlargement of the portion indicated by the dotted rectangle in *B*1 shows clearly identifiable membrane hyperpolarization (about −5 mV) during exposure to extracellular Cs^+. *B*3, enlargements of the voltage responses to the hyperpolarizing current pulses before, during and after the bath application of Cs^+. Traces are from the points indicated by *a, b* and *c* in *B*1. The oblique arrows point to the voltage 'sag'. Note that the blockade and recovery of the voltage 'sag' is coincident with the membrane potential (V_m) changes.

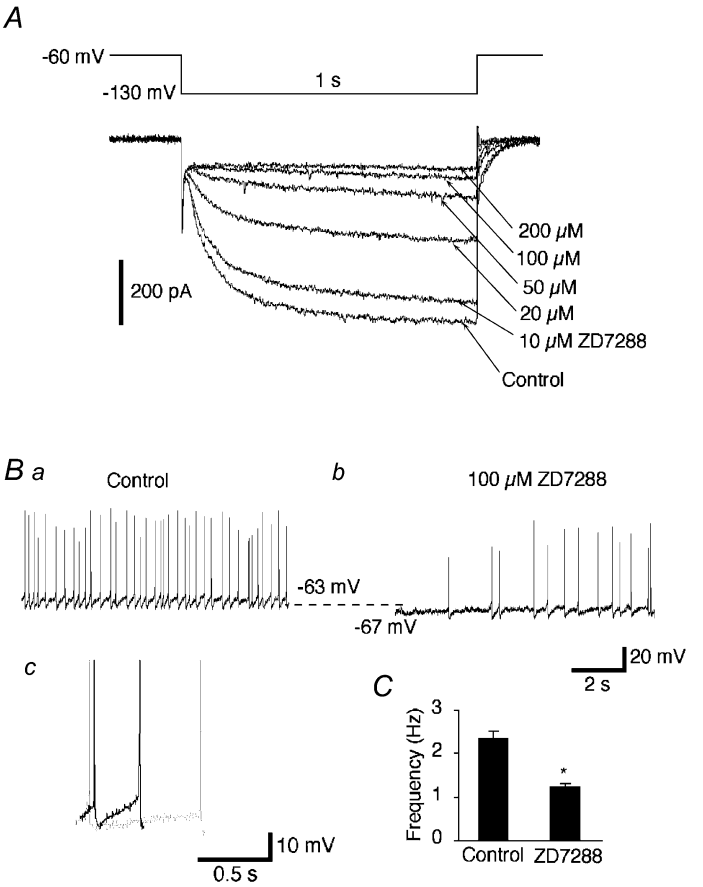

Figure 5. Sensitivity of I_h to ZD7288

A, currents elicited by hyperpolarizing voltage steps (1 s duration, from −60 to −130 mV) before and during the bath application of ZD7288 (10–200 μM). *B*, spontaneous discharges recorded in the current-clamp mode before (*Ba*) and during (*Bb*) the bath application of ZD7288 (100 μM). Note that ZD7288 induced a marked decrease in the spontaneous discharge rate and the membrane hyperpolarization (about 4 mV). *Bc*, the trajectory of the slow depolarization between two spikes before (dark trace) and during (light trace) the application of ZD7288. Note that blockade of I_h by ZD7288 caused a slower time course of the depolarization towards the second spike. *C*, mean values for the frequency of action potentials before and during the application of ZD7288 (*$P < 0.01$, $n = 6$).

change may have resulted from the effects of I_h blockade on the resting membrane potential. ZD7288 caused a membrane potential decrease of about 4 mV, similar to the change caused by Cs^+ ions.

To address the question of whether firing rate changes were due entirely to membrane potential changes, we tested five cells in a similar fashion to that described above, but with constant current injection to compensate for changes in resting membrane potential. We tested five cells that did not show spontaneous firing at rest by holding their membrane potentials at depolarized potentials to cause firing. As shown in Fig. 6, we made a comparison between the action potentials generated during the control condition (which included DC current injection to cause firing) and action potentials generated in the presence of ZD7288. The frequency of action potentials significantly

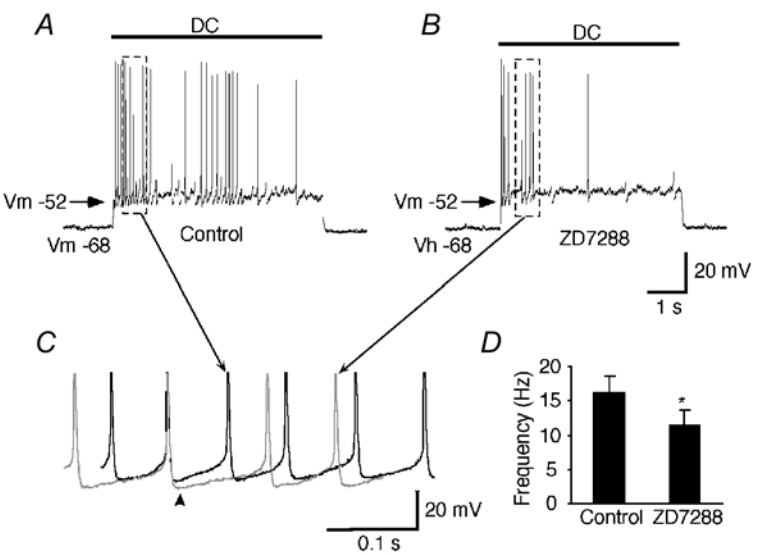

Figure 6. Effects of ZD7288 on the generation of action potentials

Repetitive action potentials generated by artificial membrane depolarization using DC current injection before (*A*) and after (*B*) the bath application of ZD7288 (100 μM). The intensity of the injected DC current was adjusted to produce the same depolarized membrane potential (e.g. holding potential, $V_h = -52$ mV). ZD7288-induced hyperpolarization was compensated by continuous DC current injection to hold the membrane potential at the value of the initial resting level (e.g. −68 mV). *C*, enlargements of the portion indicated by the dashed rectangle in *A* and *B*. Traces were superimposed according to their firing threshold. Note an increase in the AHP amplitude and the prolonged time course of the AHP phase (arrowhead). *D*, mean values for the frequency of action potentials before and during the application of ZD7288 (*$P < 0.01$, $n = 5$).

decreased by 32.8 ± 7.2 % in the presence of ZD7288 ($P < 0.01$, $n = 5$, Fig. 6*D*), even though the membrane potential was held at the pre-drug level. By superimposing action potentials generated in the presence and absence of ZD7288, we found increases in both the AHP amplitude and its duration (Fig. 6*C*, arrowhead). The difference between peak amplitudes of AHP was −2.1 ± 0.2 mV ($n = 9$ epochs in each). Given that the activation range of I_h in area postrema neurons is between −60 and −130 mV (Funahashi *et al.* 2002*b*), the AHP may activate a much smaller I_h at membrane potentials around −52 mV than those closer to the normal resting revel (e.g. −68 mV). The mechanism of ZD7288-induced decreases in the firing frequency at the membrane potentials around −52 mV could not be explained by the changes in the slope of slow depolarization. The mean values for the slope steepness in this cell before and during the application of ZD7288 were 110 ± 8 to 118 ± 11, respectively ($n = 7$ epochs in each). The mean values for the slope steepness changed to 95 ± 5 % of the control level during the application of ZD7288 ($n = 5$ cells). The change in the slope steepness was not statistically significant ($P > 0.05$, $n = 5$ cells). In contrast with the changes in AHP shape that were shown in response to ZD7288 when the membrane potential was permitted to change (Fig. 5*B*), no significant changes were found in the course of slow depolarization during the AHP when the membrane potential changes induced by ZD7288 were compensated. These results indicate that I_h contributes to the regulation of the spontaneous discharge rate by multiple mechanisms: an effect on resting potential and effects on after-potential properties.

Effects of I_h activation on rebound potentials

Area postrema cells displaying I_h typically showed rebound potentials that could reach firing threshold at the termination of hyperpolarizing step pulses (Fig. 7). As shown in Fig. 7*A*, blockade of I_h by the application of ZD7288 changed the time course of the rebound potential, resulting in a longer latency of the rebound action potentials (from 6.1 ± 0.2 ms to 15.4 ± 1.1 ms, $P < 0.01$, $n = 7$). In normal ACSF, the latency of the first rebound action potential was quite stable (1.7 ± 0.4 ms jitter; $n = 9$), even when cells were held at different membrane

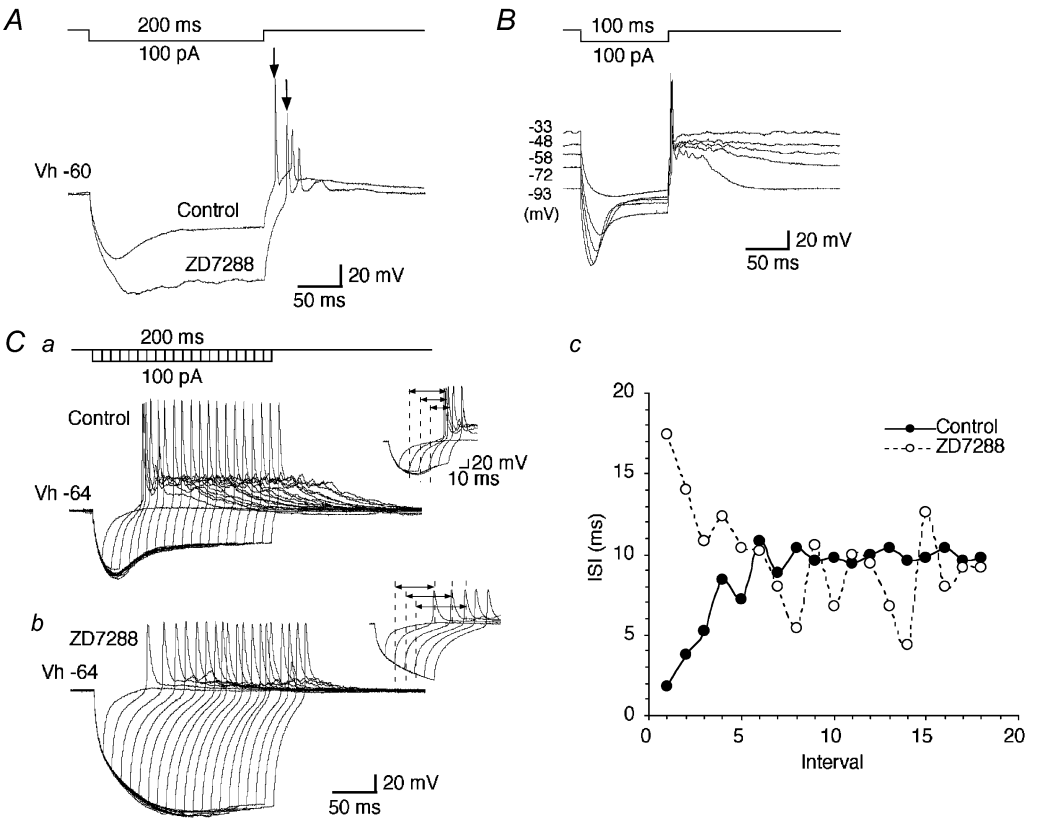

Figure 7. I_h stabilizes the timing of rebound action potentials

A, voltage responses to the current injection as indicated before and during the application of ZD7288 (100 μM). Note the longer latency of the rebound action potentials. *B*, voltage responses to the current injection as indicated at different membrane potentials. The resting potential was −58 mV. Note the stable latency of the first rebound action potentials. *C*, effect of time-dependent activation and deactivation of I_h on rebound action potential generation before (*Ca*) and during (*Cb*) the application of ZD7288 (100 μM). Voltage steps: 100 pA, up to 200 ms duration with 10 ms increment. Insets show the enlargement of initial several rebound action potentials in each condition. *Cc*, plots of the values for the ISI against the number of each interval before (●) and during (○) the application of ZD7288.

potentials over a wide range (Fig. 7*B*). These data suggested that small activation of I_h was enough to stabilize the timing of the rebound action-potential generation. As the I_h is activated in a time-dependent manner, we next examined the effect of changes in the duration of the hyperpolarizing step pulses on the latency of rebound action potentials (Fig. 7*Ca* and *b*). Rebound action potentials were triggered when the duration of hyperpolarizing step pulses (100 pA) increased to 20 ms or more. The latency of rebound action potentials gradually decreased in the early phase and the interspike interval (ISI) was stabilized in the later phase in the control condition, whereas in the presence of ZD7288 the latency of rebound action potentials increased in the early phase and the ISI still fluctuated in the later phase (Fig. 7*Ca* and *b*, insets, and *c*; $n = 4$). These results suggest that I_h could contribute to the periodicity of the generation of action potentials.

Ba^{2+} does not block I_h

Extracellular Ba^{2+} has been reported to suppress I_{Kir} and the leak conductance with a relatively small influence on I_h (Halliwell & Adams, 1982; McCormick & Pape, 1990*a*; Womble & Moises, 1993; Bayliss *et al.* 1994; Zidichouski & Jhamandas, 1999; Kilb & Luhmann, 2000; Thoby-Brisson *et al.* 2000). We sought to determine the effect of Ba^{2+} on I_h in the area postrema. The bath application of $BaCl_2$ (1 mM) produced a marked inward shift of the holding current and a decrease in the leak conductance (I_{in}), but no significant changes in the amplitude of I_h, as measured by the difference between I_{ss} and I_{in} (Fig. 8*A* and *B*, $n = 7$). The effect of Ba^{2+} on the resting potential was in the opposite direction to the effects of Cs^+ and ZD7288 (Fig. 8*C* and *D*, $n = 5$). Voltage recordings in current-clamp mode showed a depolarization of the membrane potential by an average of 12.6 ± 1.5 mV ($n = 8$) and an increase in the input resistance up to 163 ± 9 % of the control level ($P < 0.01$, $n = 4$), although the magnitude of the voltage 'sag' increased by 6.1 ± 1.6 % ($P < 0.05$, $n = 4$). Some cells showed a transient increase in the spontaneous discharge rate at the beginning of the application of $BaCl_2$ (data not shown). A similar effect of Ba^{2+} has been reported in cells displaying I_{Kir} (Flynn *et al.* 1999). From these findings, we concluded that external Ba^{2+} does not block the I_h in area postrema

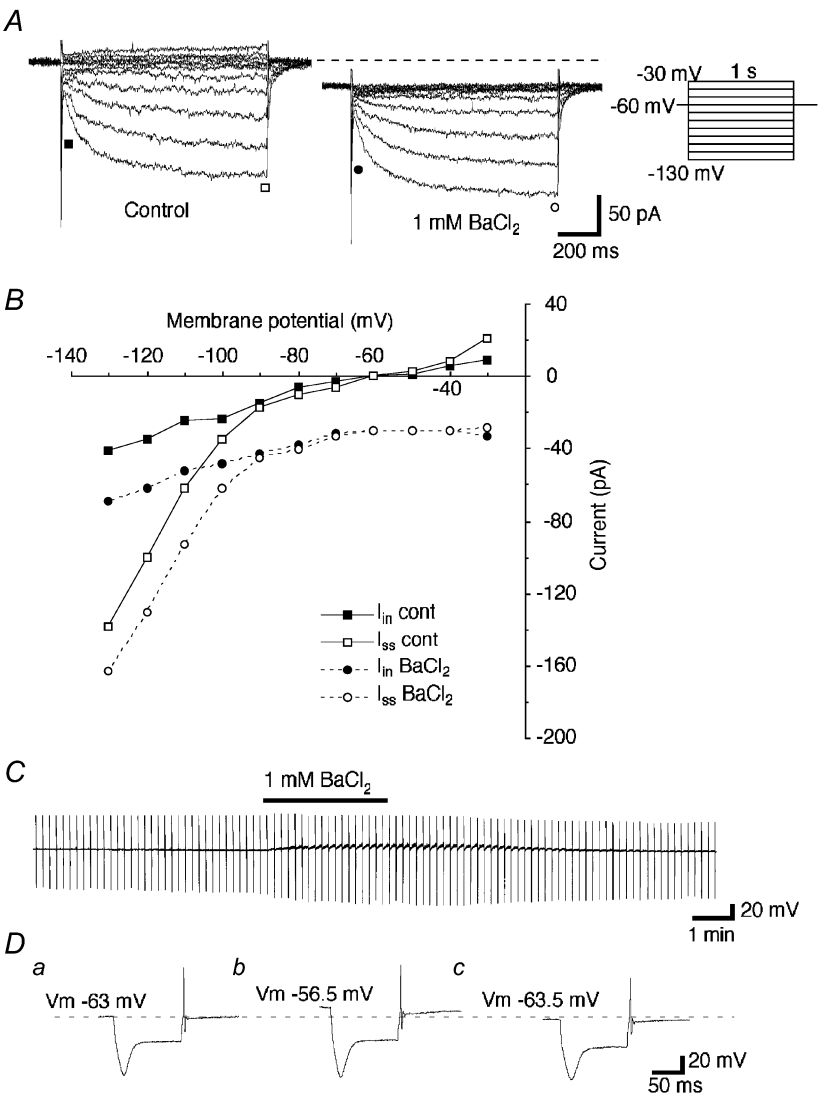

Figure 8. Extracellular Ba^{2+} does not block I_h

A, currents elicited by hyperpolarizing voltage steps (1 s duration, from −30 to −130 mV with 10 mV decrements) before and during the bath application of $BaCl_2$ (1 mM). *B*, plots of I_{in} (■) and I_{ss} (□) in the control medium, and I_{in} (●) and I_{ss} (○) during the application of $BaCl_2$. Note that extracellular Ba^{2+} caused a marked inward shift of the holding current and a slight decrease in the leak conductance, but no significant change in the amplitude of I_h. *C*, recordings of the membrane potential and input resistances before, during and after the bath application of $BaCl_2$ (1 mM). The thick line indicates the period of the application of $BaCl_2$. A hyperpolarizing current pulse (160 pA, 100 ms duration) was injected every 10 s to monitor the input resistance changes. Note a marked membrane depolarization with an increase in the input resistance during the effect of extracellular Ba^{2+}. *D*, enlargements of the voltage responses to the hyperpolarizing current pulses before (*a*), during (*b*) and after (*c*) the bath application of $BaCl_2$.

neurons; rather, a possible blockade of I_{Kir}-like channels may account for the depolarization of the membrane potential during the application of $BaCl_2$.

Modulation of I_h by intracellular cAMP

Finally, we examined the regulation of I_h by cAMP. To avoid washing out the cytoplasmic biochemicals required for second-messenger-mediated responses, perforated patch recordings were performed using amphotericin B. In whole-cell recordings, no significant increase was observed in the amplitude of I_h during the bath application of the membrane-permeable analogue of cAMP 8Br-cAMP (up to 1 mM, $n = 8$) or the adenylate cyclase activator forskolin (up to 100 μM, $n = 7$). As shown in Fig. 9*A*, in perforated patch recordings, bath application of 8Br-cAMP (1 mM) increased the amplitude of I_h by an average of 5.3 ± 1.4 % ($P < 0.05$, $n = 7$). The value of $V_{½}$ shifted by an average of 2.5 ± 0.4 mV ($P < 0.05$, $n = 7$) in the positive direction (Fig. 9*B*). This positive shift induced by cAMP was similar to that reported for HCN1-type channels, and different from that reported for HCN2 or native I_h channels in thalamic neurons (Biel *et al.* 1999). The application of forskolin (50–100 μM) caused a slight increase of the amplitude of I_h (i.e. always less than the increase caused by 1 mM 8Br-cAMP; $n = 4$). To test whether physiological changes in intracellular cAMP concentration were enough to cause maximal activation of I_h channels, we bath applied the adenylate cyclase inhibitor SQ22536 (50 μM, see Fabbri *et al.* 1991). SQ22536 caused no significant changes in the amplitude or activation curves of I_h ($n = 6$). The amplitude of I_h was changed to 100.4 ± 3.8 % of the control level ($P > 0.05$, $n = 6$). The value of $V_{½}$ was changed from −96.8 ± 0.4 to 96.4 ± 0.3 mV ($P > 0.05$, $n = 6$). From these results, we concluded that I_h in area postrema neurons is only weakly modulated by the intracellular cAMP system.

DISCUSSION

The cells displaying the hyperpolarization-activated cation current (I_h) formed a major fraction of rat area postrema neurons in 160 of 255 cells tested in the present study. Their intrinsic membrane properties were characterized by a marked voltage 'sag' in response to hyperpolarizing pulses in current-clamp mode. The properties of I_h demonstrated in the present study are: (1) the dependence of its amplitude on the transmembrane Na^+ and K^+ gradients, (2) its blockade by external Cs^+ and ZD7288, but not Ba^{2+} and (3) a weak activation by intracellular cAMP. Finally, we demonstrate a functional role for I_h in the pacemaking of action potentials in area postrema neurons.

Properties of I_h in area postrema neurons

The reversal potential (approximately −36 mV) of I_h in area postrema neurons was consistent with a mixed Na^+ and K^+ permeability (Figs 2 and 3) and was close to the reversal potential values reported for I_h in other central neurons (Halliwell & Adams, 1982; McCormick & Pape, 1990*a*; Bayliss *et al.* 1994; Maccaferri & McBain, 1996). A contribution to I_h by K^+ ions was clearly apparent when I_h was activated at membrane potentials more negative than E_K (< −100 mV). As shown in Fig. 2*A* and *B*, an increment in the conductance on changing from 5 to 20 mM $[K^+]_o$ was greater than the value that was estimated from the change in the driving force of K^+, even if a certain amount of Goldman-type rectification was considered. Previous studies reported that external K^+ increased the Na^+ conductance of I_h (Hestrin, 1987; Frace *et al.* 1992). It was also suggested that I_h channels have multiple ion binding

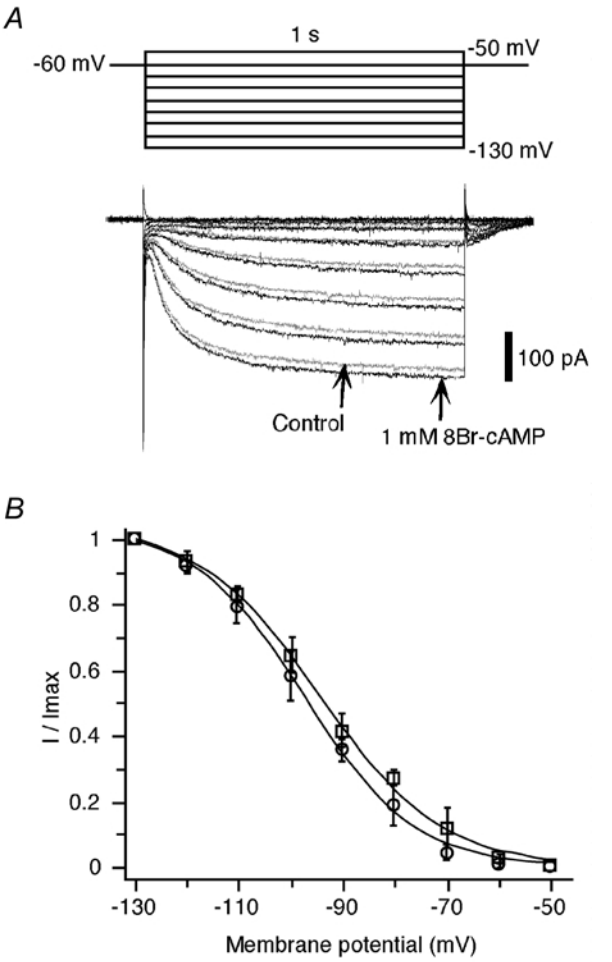

Figure 9. Weak modulation of I_h by intracellular cAMP

A, currents elicited by hyperpolarizing voltage steps (1 s duration, from −50 to −130 mV with 10 mV decrements) before (grey) and during (black) the bath application of 8Br-cAMP (1 mM). Note a slight increase in the amplitude of I_h induced by 8Br-cAMP at millimolar concentrations. *B*, activation curve of the conductance underlying I_h constructed with plots of the mean normalized tail currents as a function of the membrane potential before (○) and during (□) the application of 8Br-cAMP ($n = 7$ cells in each). Each of the resulting values was fitted to the Boltzmann equation and yielded an activation with $V_{½} = -97.5 \pm 0.8$ and -94.6 ± 0.9 mV, $k = 10.5 \pm 0.6$ and 11.6 ± 0.6, before and during the application of 8Br-cAMP, respectively.

sites that showed differential affinity for K^+ and Na^+ (DiFrancesco, 1982; Wollmuth, 1995). There may be a potential mechanism for extracellular K^+ to affect the gating of the I_h channel; however, this remains to be determined.

It has been suggested that I_h contributes to the production of the AHP that follows action potentials (McCormick & Pape, 1990*a*; Maccaferri *et al.* 1993). As reported in our previous paper (Funahashi *et al.* 2002*b*), the AHP was enhanced when cells were held at relatively negative membrane potentials (i.e. within the activation range of I_h). This suggested that substantial activation of I_h occurs during the AHP. In the present study, ZD7288, a specific blocker of I_h, only changed the trajectory of the slow depolarization between two spontaneous action potentials (Fig. 5*B*). In addition, we showed an increase in the peak amplitude of AHP during the application of ZD7288 when cells were held at their resting potentials (Fig. 6*C*). These findings indicate that the AHP is primarily produced by other currents, such as a Ca^{2+}-activated K^+ current. In physiological conditions, the AHP following one action potential, mediated by a Ca^{2+}-activated K^+ current, can send a cell's membrane potential into the activation range of I_h. An activation of I_h would then increase the likelihood for generating another action potential. We suggest that I_h can control the rate of spontaneous firing in area postrema neurons in a manner that is similar to its role in cardiac tissues (DiFrancesco, 1991).

Modulation of I_h by cAMP and suggestions for channel types involved

Recently, the molecular identification of genes encoding I_h channels has enabled studies of the electrophysiological properties of specific channel types that mediate an I_h. Among the HCN channel family (HCN1–HCN4), the HCN1 channel subtype has been shown to be much less sensitive to the intracellular concentration of cAMP than the HCN2 channel subtype (Biel *et al.* 1999). The half-activation concentration of cAMP for HCN2 channels is 0.5 μM (Ludwig *et al.* 1998). In the present study, we showed that a relatively high concentration of 8Br-cAMP (1 mM) caused a slight increase in the amplitude of I_h with a positive shift of the voltage dependence. Forskolin caused smaller effects on I_h than those induced by a high concentration of 8Br-cAMP. These results suggested that the sensitivity of the I_h channel subtype in area postrema neurons to intracellular cAMP could be much less than that of HCN2 channels. We also found that there were no significant changes in either the amplitude or the activation kinetics of I_h during the application of SQ22536, suggesting that the likelihood of tonic upregulation of I_h channels by the intracellular cAMP system is even smaller.

HCN1 channels showed a substantially faster time course of activation than HCN2 and HCN3 channels (Moosmang *et al.* 2001). We previously showed that the time course and $V_{½}$ of I_h activation in area postrema neurons was similar to the behaviour of channels in hippocampal CA1 neurons, which also suggests that I_h may be mediated by the HCN1 channel subtype (Funahashi *et al.* 2002*b*). None of the cells tested in our present and previous studies showed a substantially slower activation time constant. This suggests that the HCN1/HCN3 expression ratio may be quite uniform in individual area postrema neurons.

Finally, the differences in the sensitivity to cAMP and the time course of activation obtained from cloned HCN channels parallel differences in the distribution of specific channel types in the brain. Studies using *in situ* hybridization of native HCN channels have shown that HCN1 expression is restricted to limited regions of the brain such as hippocampal CA1 neurons, while HCN2 is highly expressed in thalamic neurons (Biel *et al.* 1999; Monteggia *et al.* 2000).

The functional role of I_h in the area postrema

Among the various autonomic responses, decreases in blood pressure and heart rate are elicited by electrical stimulation in the rat area postrema, indicating a clear relationship between outputs from the area postrema and autonomic activity (Ferguson & Smith, 1991). Since I_h in area postrema neurons can be weakly modulated by the cAMP system, any chemical substances or neurotransmitters that alter cAMP levels will have a small effect on resting potential, spontaneous activity and rebound potential latency. This feature of I_h may stabilize spontaneous discharge rates in area postrema neurons.

In contrast to these compounds, ZD7288, which was originally produced as a bradycardic agent, and anaesthetics such as enflurane, halothane and propofol can directly reduce the I_h conductance (Tokimasa *et al.* 1990; Funahashi *et al.* 2001). These drugs should induce a hyperpolarization of membrane potential, a decrease in the slope steepness of slow depolarization and a longer latency of rebound action potentials. As a result, the spontaneous discharge rate of area postrema neurons should decrease when area postrema neurons are exposed to these drugs. I_h may also prevent excessive hyperpolarization of cells by synaptic inputs or direct receptor activation by chemical substances. Further investigation will be required to establish the relationship between the excitability of a specific subpopulation of area postrema neurons and each autonomic function.

In conclusion, the results of the present study suggest that I_h plays an important role in pacemaking the generation of action potentials and regulation of the resting membrane potential of neurons in the area postrema. Such an intrinsic mechanism enables the majority of area postrema neurons to maintain a certain spontaneous discharge rate. These cells could provide tonic synaptic input onto their target cells. An understanding of the firing properties of

area postrema neurons and the intrinsic (e.g. I_h channels) and extrinsic (e.g. chemicals or transmitters that may alter cAMP levels) factors that control such firing will be essential for any understanding of the physiological roles of area postrema neurons.

REFERENCES

Allen MA & Ferguson AV (1996). *In vitro* recordings from area postrema neurons demonstrate responsiveness to adrenomedullin. *Am J Physiol* **270**, R920–925.

Barnes KL, Knowles WD & Ferrario CM (1988). Neuronal responses to angiotensin II in the *in vitro* slice from the canine medulla. *Hypertension* **11**, 680–684.

Bayliss DA, Viana F, Bellingham MC & Berger AJ (1994). Characteristics and postnatal development of a hyperpolarization-activated inward current in rat hypoglossal motoneurons *in vitro*. *J Neurophysiol* **71**, 119–128.

Berger BD, Wise CD & Stein L (1973). Area postrema damage and bait shyness. *J Comp Physiol Psychol* **82**, 475–479.

Biel M, Ludwig A, Zong X & Hofmann F (1999). Hyperpolarization-activated cation channels: a multi-gene family. *Rev Physiol Biochem Pharmacol* **136**, 165–181.

Borison HL & Wang SC (1953). Physiology and pharmacology of vomiting. *Pharmacol Rev* **5**, 193–230.

BoSmith RE, Briggs I & Sturgess NC (1993). Inhibitory actions of ZENECA ZD7288 on whole-cell hyperpolarization activated inward current (If) in guinea-pig dissociated sinoatrial node cells. *Br J Pharmacol* **110**, 343–349.

Brown HF, Giles W & Noble SJ (1977). Membrane currents underlying activity in frog sinus venosus. *J Physiol* **271**, 783–816.

Carpenter DO, Briggs DB, Knox AP & Strominger N (1988). Excitation of area postrema neurons by transmitters, peptides, and cyclic nucleotides. *J Neurophysiol* **59**, 358–369.

Coil JD & Norgren R (1981). Taste aversions conditioned with intravenous copper sulfate: attenuation by ablation of the area postrema. *Brain Res* **212**, 425–433.

Contreras RJ, Kosten T & Bird E (1984). Area postrema: part of the autonomic circuitry of caloric homeostasis. *Fed Proc* **43**, 2966–2968.

Dickson CT, Magistretti J, Shalinsky MH, Fransen E, Hasselmo ME & Alonso A (2000). Properties and role of I(h) in the pacing of subthreshold oscillations in entorhinal cortex layer II neurons. *J Neurophysiol* **83**, 2562–2579.

DiFrancesco D (1981). A new interpretation of the pace-maker current in calf Purkinje fibres. *J Physiol* **314**, 359–376.

DiFrancesco D (1982). Block and activation of the pace-maker channel in calf purkinje fibres: effects of potassium, caesium and rubidium. *J Physiol* **329**, 485–507.

DiFrancesco D (1991). The contribution of the 'pacemaker' current (i_f) to generation of spontaneous activity in rabbit sino-atrial node myocytes. *J Physiol* **434**, 23–40.

Fabbri E, Brighenti L & Ottolenghi C (1991). Inhibition of adenylate cyclase of catfish and rat hepatocyte membranes by 9-(tetrahydro-2-furyl)adenine (SQ 22536). *J Enzyme Inhib* **5**, 87–98.

Ferguson AV & Smith P (1991). Autonomic mechanisms underlying area postrema stimulation-induced cardiovascular responses in rats. *Am J Physiol* **261**, R1–8.

Flynn ER, McManus CA, Bradley KK, Koh SD, Hegarty TM, Horowitz B & Sanders KM (1999). Inward rectifier potassium conductance regulates membrane potential of canine colonic smooth muscle. *J Physiol* **518**, 247–256.

Frace AM, Maruoka F & Noma A (1992). External K^+ increases Na^+ conductance of the hyperpolarization-activated current in rabbit cardiac pacemaker cells. *Pflugers Arch* **421**, 97–99.

Funahashi M & Adachi A (1993). Glucose-responsive neurons exist within the area postrema of the rat: *in vitro* study on the isolated slice preparation. *Brain Res Bull* **32**, 531–535.

Funahashi M, Higuchi H, Miyawaki T, Shimada M & Matsuo R (2001). Propofol suppresses a hyperpolarization-activated inward current in rat hippocampal CA1 neurons. *Neurosci Lett* **311**, 177–180.

Funahashi M, Mitoh Y & Matsuo R (2002*a*). Two distinct types of transient outward currents in area postrema neurons in rat brain slices. *Brain Res* **942**, 31–45.

Funahashi M, Mitoh Y & Matsuo R (2002*b*). Electrophysiological properties of the rat area postrema neurons displaying both the transient outward current and the hyperpolarization-activated inward current. *Brain Res Bull* **58**, 337–343.

Gallo M, Arnedo M, Aguero A & Puerto A (1990). The functional relevance of the area postrema in drug-induced aversion learning. *Pharmacol Biochem Behav* **35**, 543–551.

Gasparini S & DiFrancesco D (1997). Action of the hyperpolarization-activated current (I_h) blocker ZD 7288 in hippocampal CA1 neurons. *Pflugers Arch* **435**, 99–106.

Halliwell JV & Adams PR (1982). Voltage-clamp analysis of muscarinic excitation in hippocampal neurons. *Brain Res* **250**, 71–92.

Harris NC & Constanti A (1995). Mechanism of block by ZD 7288 of the hyperpolarization-activated inward rectifying current in guinea pig substantia nigra neurons *in vitro*. *J Neurophysiol* **74**, 2366–2378.

Hay M, Hasser EM & Lindsley KA (1996). Area postrema voltage-activated calcium currents. *J Neurophysiol* **75**, 133–141.

Hay M & Lindsley KA (1995). Membrane properties of area postrema neurons. *Brain Res* **705**, 199–208.

Hestrin S (1987). The properties and function of inward rectification in rod photoreceptors of the tiger salamander. *J Physiol* **390**, 319–333.

Iovino M, Papa M, Monteleone P & Steardo L (1988). Neuroanatomical and biochemical evidence for the involvement of the area postrema in the regulation of vasopressin release in rats. *Brain Res* **447**, 178–182.

Jahn K, Bufler J, Weindl A, Arzberger T & Hatt H (1996). Patch-clamp study on membrane properties and transmitter activated currents of rabbit area postrema neurons. *J Comp Physiol A* **178**, 771–778.

Kilb W & Luhmann HJ (2000). Characterization of a hyperpolarization-activated inward current in Cajal-Retzius cells in rat neonatal neocortex. *J Neurophysiol* **84**, 1681–1691.

Li Z & Hay M (2000). 17-Beta-estradiol modulation of area postrema potassium currents. *J Neurophysiol* **84**, 1385–1391.

Ludwig A, Zong X, Jeglitsch M, Hofmann F & Biel M (1998). A family of hyperpolarization-activated mammalian cation channels. *Nature* **393**, 587–591.

Luthi A & McCormick DA (1998). H-current: properties of a neuronal and network pacemaker. *Neuron* **21**, 9–12.

Maccaferri G, Mangoni M, Lazzari A & DiFrancesco D (1993). Properties of the hyperpolarization-activated current in rat hippocampal CA1 pyramidal cells. *J Neurophysiol* **69**, 2129–2136.

Maccaferri G & McBain CJ (1996). The hyperpolarization-activated current (I_h) and its contribution to pacemaker activity in rat CA1 hippocampal stratum oriens-alveus interneurones. *J Physiol* **497**, 119–130.

McCormick DA & Pape HC (1990*a*). Noradrenergic and serotonergic modulation of a hyperpolarization-activated cation current in thalamic relay neurones. *J Physiol* **431**, 319–342.

McCormick DA & Pape HC (1990*b*). Properties of a hyperpolarization-activated cation current and its role in rhythmic oscillation in thalamic relay neurones. *J Physiol* **431**, 291–318.

Miselis RR, Shapiro RE & Hyde TM (1987). The area postrema. In *Circumventricular Organs and Body Fluids*, vol. II, ed. Gross P, pp. 185–207. CRC, Boca Raton, FL, USA.

Monteggia LM, Eisch AJ, Tang MD, Kaczmarek LK & Nestler EJ (2000). Cloning and localization of the hyperpolarization-activated cyclic nucleotide-gated channel family in rat brain. *Brain Res Mol Brain Res* **81**, 129–139.

Moosmang S, Stieber J, Zong X, Biel M, Hofmann F & Ludwig A (2001). Cellular expression and functional characterization of four hyperpolarization-activated pacemaker channels in cardiac and neuronal tissues. *Eur J Biochem* **268**, 1646–1652.

Pape HC (1992). Adenosine promotes burst activity in guinea-pig geniculocortical neurones through two different ionic mechanisms. *J Physiol* **447**, 729–753.

Pape HC (1996). Queer current and pacemaker: the hyperpolarization-activated cation current in neurons. *Annu Rev Physiol* **58**, 299–327.

Rae J, Cooper K, Gates P & Watsky M (1991). Low access resistance perforated patch recordings using amphotericin B. *J Neurosci Methods* **37**, 15–26.

Ritter RC, Edwards GE & Nonavinakere VK (1986). Hindbrain control of food intake: behavioral evidence for metabolic sensing and modulation of orosensory responsiveness. In *Emotions*, ed. Oomura Y, pp. 137–148. Japan Scientific Societies Press, Tokyo.

Santoro B, Chen S, Luthi A, Pavlidis P, Shumyatsky GP, Tibbs GR & Siegelbaum SA (2000). Molecular and functional heterogeneity of hyperpolarization-activated pacemaker channels in the mouse CNS. *J Neurosci* **20**, 5264–5275.

Thoby-Brisson M, Telgkamp P & Ramirez JM (2000). The role of the hyperpolarization-activated current in modulating rhythmic activity in the isolated respiratory network of mice. *J Neurosci* **20**, 2994–3005.

Tokimasa T, Sugiyama K, Akasu T & Muteki T (1990). Volatile anaesthetics inhibit a cyclic AMP-dependent sodium-potassium current in cultured sensory neurones of bullfrog. *Br J Pharmacol* **101**, 190–192.

Travagli RA & Gillis RA (1994). Hyperpolarization-activated currents, I_H and I_{KIR}, in rat dorsal motor nucleus of the vagus neurons *in vitro*. *J Neurophysiol* **71**, 1308–1317.

Van Der Kooy D (1984). Area postrema: site where cholecystokinin acts to decrease food intake. *Brain Res* **295**, 345–347.

Wollmuth LP (1995). Multiple ion binding sites in I_h channels of rod photoreceptors from tiger salamanders. *Pflugers Arch* **430**, 34–43.

Womble MD & Moises HC (1993). Hyperpolarization-activated currents in neurons of the rat basolateral amygdala. *J Neurophysiol* **70**, 2056–2065.

Yanagihara K & Irisawa H (1980). Potassium current during the pacemaker depolarization in rabbit sinoatrial node cell. *Pflugers Arch* **388**, 255–260.

Zidichouski JA & Jhamandas JH (1999). Characterization of a hyperpolarizing-activated current in rat lateral parabrachial neurons. *Neurosci* **89**, 863–871.

Acknowledgements

We thank Dr Mark Stewart (SUNY Downstate Medical Center, Brooklyn, NY, USA) for his helpful comments on the manuscript. This research was partly supported by grants from the Ministry of Education, Science and Culture of Japan, Novartis foundation (Japan) for the Promotion of Science, Kato Memorial Bioscience Foundation and Kobayashi Magobei Memorial Foundation.